Acta Cryst E CRYSTALLOGRAPHIC COMMUNICATIONS
ISSN 2056-9890

A new monoclinic polymorph of *N*-(3-methylphenyl)ethoxycarbothioamide: crystal structure and Hirshfeld surface analysis

Mukesh M. Jotani,[a]‡ Chien Ing Yeo[b] and Edward R. T. Tiekink[b]*

[a]Department of Physics, Bhavan's Sheth R. A. College of Science, Ahmedabad, Gujarat 380 001, India, and [b]Research Centre for Crystalline Materials, School of Science and Technology, Sunway University, 47500 Bandar Sunway, Selangor Darul Ehsan, Malaysia. *Correspondence e-mail: edwardt@sunway.edu.my

Received 9 November 2017
Accepted 12 November 2017

Edited by W. T. A. Harrison, University of Aberdeen, Scotland

‡ Additional correspondence author, e-mail: mmjotani@rediffmail.com.

Keywords: crystal structure; carbothioamide; hydrogen bonding; Hirshfeld surface analysis.

CCDC reference: 1585129

Supporting information: this article has supporting information at journals.iucr.org/e

The title compound, $C_{10}H_{13}NOS$, is a second monoclinic polymorph (space group $P2_1/c$, Z' = 2) of the previously reported $C2/c$ (Z = 1) polymorph [Tadbuppa & Tiekink (2005). *Z. Kristallogr. New Cryst. Struct.* **220**, 395–396]. Two independent molecules comprise the asymmetric unit of the new polymorph and each of these exists as a thioamide–thione tautomer. In each molecule, the central CNOS chromophore is strictly planar [r.m.s. deviations = 0.0003 and 0.0015 Å] and forms dihedral angles of 6.17 (5) and 20.78 (5)° with the N-bound 3-tolyl rings, thereby representing the major difference between the molecules. The thione-S and thioamide-N—H atoms are *syn* in each molecule and this facilitates the formation of an eight-membered thioamide $\{\cdots SCNH\}_2$ synthon between them; the dimeric aggregates are consolidated by pairwise 3-tolyl-C—H$\cdots$S interactions. In the extended structure, supramolecular layers parallel to (102) are formed *via* a combination of 3-tolyl-C—H$\cdots\pi$(3-tolyl) and weak π–π interactions [inter-centroid distance between 3-tolyl rings = 3.8535 (12) Å]. An analysis of the Hirshfeld surfaces calculated for both polymorphs reveals the near equivalence of one of the independent molecules of the $P2_1/c$ form to that in the $C2/c$ form.

1. Chemical context

Molecules of the general formula $ROC(=S)N(H)R'$ [R = alkyl, aryl], *O*-thiocarbamates, are readily prepared from the reaction of an alcohol, ROH, with an isothiocyanide derivative, $R'N{=}C{=}S$. Since the first report of the structure of EtOC(=S)N(H)Ph (Taylor & Tiekink, 1994), these molecules have attracted the interest of the crystal engineering community. This interest arises primarily because of the propensity of these molecules to form thioamide-N—H$\cdots$S(thione) hydrogen bonds (Ho *et al.*, 2005; Kuan *et al.*, 2007; Slater *et al.*, 2016) and the ability of these molecules to form co-crystals with pyridyl-like molecules (Ellis *et al.*, 2009). The neutral molecules can complex bis(phosphane)copper(I) chloride to reveal fascinating intramolecular phenyl-C—H$\cdots\pi$(quasi-chelate ring) interactions where the π-system is the hydrogen-bond mediated (CuCl$\cdots$HNCS) ring (Yeo *et al.*, 2014); intermolecular versions of C—H$\cdots\pi$(quasi-chelate ring) interactions are also known (Zukerman-Schpector *et al.*, 2016). The anions form very stable compounds with phosphanegold(I) moieties to yield luminescent materials in the solid state (Ho *et al.*, 2006) as well as potential anti-bacterial (Yeo *et al.*, 2013) and anti-cancer (Ooi *et al.*, 2017) agents. It was in the latter context that the title polymorph (I) was

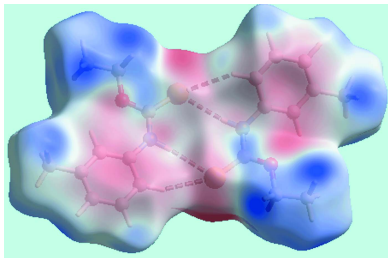

discovered. Thus, (I) was synthesized afresh for complexation to phosphanegold(I) and during characterization exhibited distinctive crystallographic properties from a previously described material, *i.e.* a *C*2/*c* form (Tadbuppa & Tiekink, 2005), hereafter (Ic). In the present report, the crystal and molecule structures of a new monoclinic polymorph of (I), *i.e.* (Ip), are described along with a Hirshfeld surface analysis of both polymorphs, conducted in order to discover distinctive packing patterns.

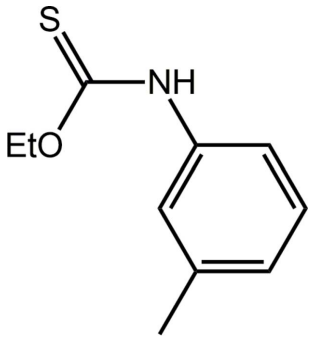

2. Structural commentary

The crystallographic asymmetric unit of (Ip), Fig. 1, comprises two independent molecules which are chemically indistinguishable, Table 1. The thione-S and thioamide-N—H atoms are *syn* in each molecule and each exists as a thioamide–thione tautomer. The central OC(=S)N chromophores are strictly planar with the r.m.s. deviation of the four fitted atoms being 0.0003 Å [0.0015 Å for the S11-molecule]. The bond lengths follow the expected trends with the C1—O1, N1 bonds being significantly shorter than the C9—O1 and C2—N1 bonds, respectively. The angles about the quaternary atom vary systematically, with those involving the thione-S1 atom being greater than the O1—C1—N1 bond angle. Of the bond angles involving the thione-S1 atom, the angle involving the O1 atom is greater by 2–3° than that formed by the sterically less encumbered N1 atom. The major difference between the key geometric parameters listed in Table 1 is found in the angles subtended at the N1 atom with the angle for the S1-molecule being nearly 3° wider than that for the S1-molecule. There is also a conformational difference between the two molecules, readily quantified in terms of the dihedral angles formed between the central chromophore and 3-tolyl rings of 6.17 (5) and 20.78 (5)° for the S1- and S11-molecules, respec-

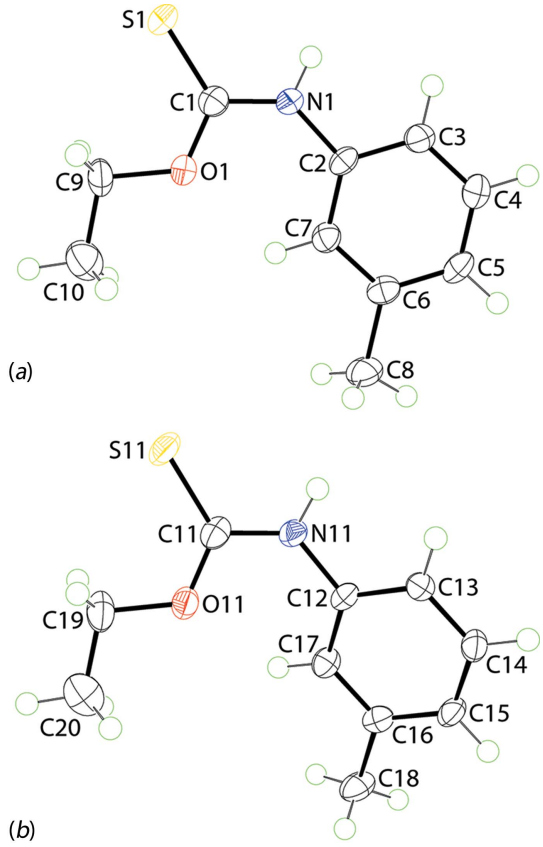

Figure 1
The molecular structures of the two independent molecules comprising the asymmetric unit of (Ip) showing the atom-labelling scheme and displacement ellipsoids at the 70% probability level.

Table 1
Selected geometric parameters (Å, °) in (Ip) and (Ic).

Parameter	(Ip), S1-molecule	(Ip), S11-molecule[a]	(Ic)
C1—S1	1.6768 (19)	1.6752 (19)	1.6720 (18)
C1—O1	1.321 (2)	1.319 (2)	1.325 (2)
C1—N1	1.338 (2)	1.339 (2)	1.337 (2)
C9—O1	1.457 (2)	1.454 (2)	1.451 (2)
C2—N1	1.421 (2)	1.423 (2)	1.426 (2)
S1—C1—O1	124.23 (14)	125.00 (15)	124.53 (12)
S1—C1—N1	122.06 (14)	121.61 (15)	122.11 (13)
O1—C1—N1	113.71 (16)	113.39 (16)	113.37 (15)
C1—O1—C9	118.72 (15)	119.01 (15)	119.29 (15)
C1—N1—C2	132.48 (16)	129.60 (16)	130.17 (15)

Note: (*a*) add 10 to atom labels to tally with the numbering in Fig. 1*b*.

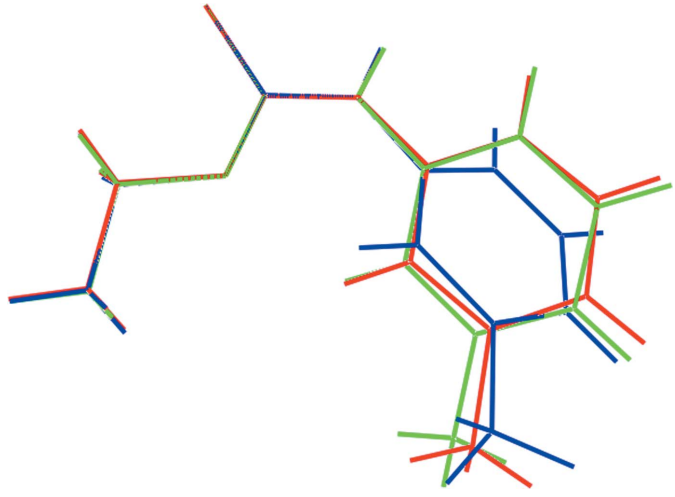

Figure 2
Overlay diagram of the two independent molecules of (Ip) (S1-molecule, red image; S11-molecule, green) and that of the original *C*2/*c* polymorph (blue image), (Ic). The molecules have been superimposed so that the central S, O and N atoms are coincident.

Table 2
Hydrogen-bond geometry (Å, °).

*Cg*1 is the centroid of the (C12–C17) ring.

D—H···*A*	*D*—H	H···*A*	*D*···*A*	*D*—H···*A*
N1—H1*N*···S11	0.87 (1)	2.62 (1)	3.4859 (16)	174 (2)
N11—H11*N*···S1	0.87 (1)	2.54 (1)	3.3985 (15)	171 (2)
C3—H3···S11	0.95	2.86	3.708 (2)	150
C13—H13···S1	0.95	2.94	3.7090 (19)	139
C17—H17···*Cg*1^{i}	0.95	2.82	3.471 (2)	127

Symmetry code: (i) $-x+2, y-\frac{1}{2}, -z+\frac{1}{2}$.

tively. As seen from the overlay diagram, Fig. 2, the ethyl groups have an open conformation and overlap closely with the C1—O1—C9—C10 and C11—O11—C19—C20 torsion angles being −178.76 (17) and 177.42 (18)°, respectively.

Geometric parameters for the original polymorph of (I), *i.e.* (Ic), are also included in Table 1. A comparison of these show the values in (Ip) and (Ic) to be equal within experimental error and those of (Ic) often lying between the two independent values found for (Ip). As evidenced from Fig. 2, there is a greater twist in the molecule as indicated by the dihedral angle of 30.44 (6)° formed between the central chromophore and the 3-tolyl ring. The orientation of the O-bound ethyl group is as for both molecules of (Ip) with the C1—O1—C9—C10 torsion angle being −176.96 (17)°.

3. Supramolecular features

The most notable feature of the molecular packing of (I) is the presence of an eight-membered thioamide synthon, {···SCNH}$_2$, formed *via* thioamide-N—H···S(thione) hydrogen bonds, between the two independent molecules comprising the asymmetric unit, Fig. 3 and Table 2. As shown in Fig. 3, the N—H···S hydrogen bonds are supported by 3-tolyl-C—H···S interactions, Table 2, with that involving the S1 atom being slightly beyond the standard distance criteria in *PLATON* (Spek, 2009). Globally, like molecules stack along the *b*-axis direction. The S1-molecules are connected *via* weak π–π interactions between the 3-tolyl rings with the inter-centroid distance being 3.8535 (12) Å for the symmetry operation $1-x, 2-y, 1-z$. The connections between the S11-molecules are of the type 3-tolyl-C—H···π(3-tolyl), Table 2. The columns pack into alternating layers of S1- and S11-molecules parallel to [001], Fig. 4*a*, and connections between them are made through the thioamide-N—H···S(thione) hydrogen bonds mentioned above, resulting in supramolecular layers parallel to (102), Fig. 4*b*. The layers, Fig. 4*c*, stack with no directional interactions between them.

The molecular packing in (Ic) has not been discussed in any detail (Tadbuppa & Tiekink, 2005) and hence, is now described. The eight-membered thioamide synthon, {···SCNH}$_2$, seen in the packing of (Ip) is also found in the packing of (Ic), Table 3, with an important difference, that being the synthon has crystallographic twofold symmetry; the putative 3-tolyl-C—H···S interaction is long at 2.92 Å.

Table 3
Hydrogen-bond geometry (Å, °) for (Ic).

*Cg*1 is the centroid of the (C2–C7) ring.

D—H···A	D—H	H···A	D···A	D—H···A
N1—H1n···S1^{i}	0.87	2.58	3.4142 (16)	160
C7—H7···*Cg*1^{ii}	0.94	2.91	3.4973 (17)	122

Symmetry code: (i) $-x, y, \frac{1}{2}-z$; (ii) $\frac{1}{2}-x, -\frac{1}{2}+y, \frac{1}{2}-z$.

Globally, molecules pack into columns parallel to the *b* axis and are sustained by 3-tolyl-C—H···π(3-tolyl) interactions, Fig. 4*d* and Table 3. Connections between columns are made by the aforementioned thioamide-N—H···S(thione) hydrogen bonds. The result is supramolecular layers that stack along the *c* axis, Fig. 4*e*. A view of the layer is shown in Fig. 4*f*.

From the images of Fig. 4, it is obvious that despite some similarities, the molecular packing in polymorphs (Ip) and (Ic) are distinct. This point is highlighted in the analysis of the Hirshfeld surfaces of (Ip) and (Ic) discussed in the next section.

4. Analysis of the Hirshfeld surfaces of (Ip) and (Ic)

The Hirshfeld surfaces for the individual molecules in (Ip), overall (Ip) and for (Ic) were calculated in accord with a recent report on a pair of polymorphs (Kuan *et al.*, 2017). The calculations clearly reveal the similarities and differences in

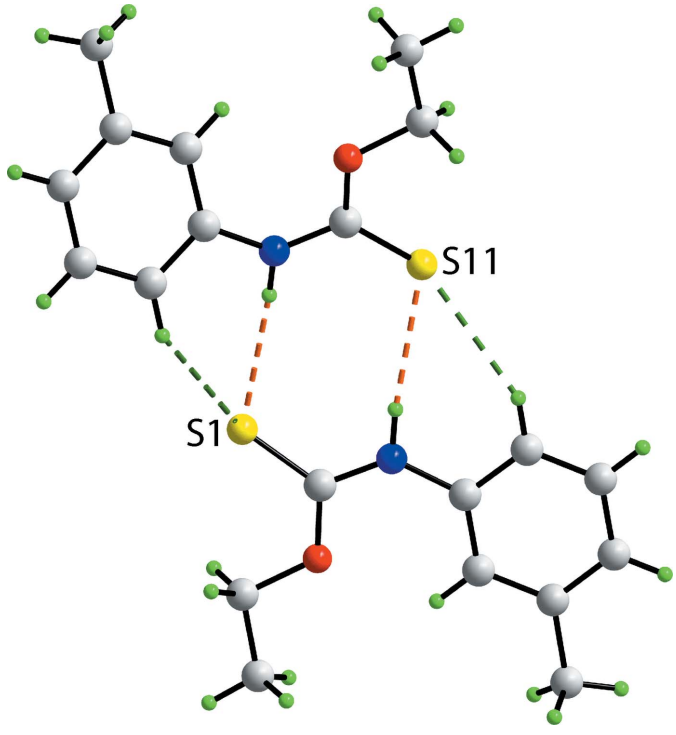

Figure 3
A view of the supramolecular dimer in (Ip) sustained by thioamide-N—H···S(thione) hydrogen bonds and supported by 3-tolyl-C—H···S(thione) interactions, shown as orange and green dashed lines, respectively.

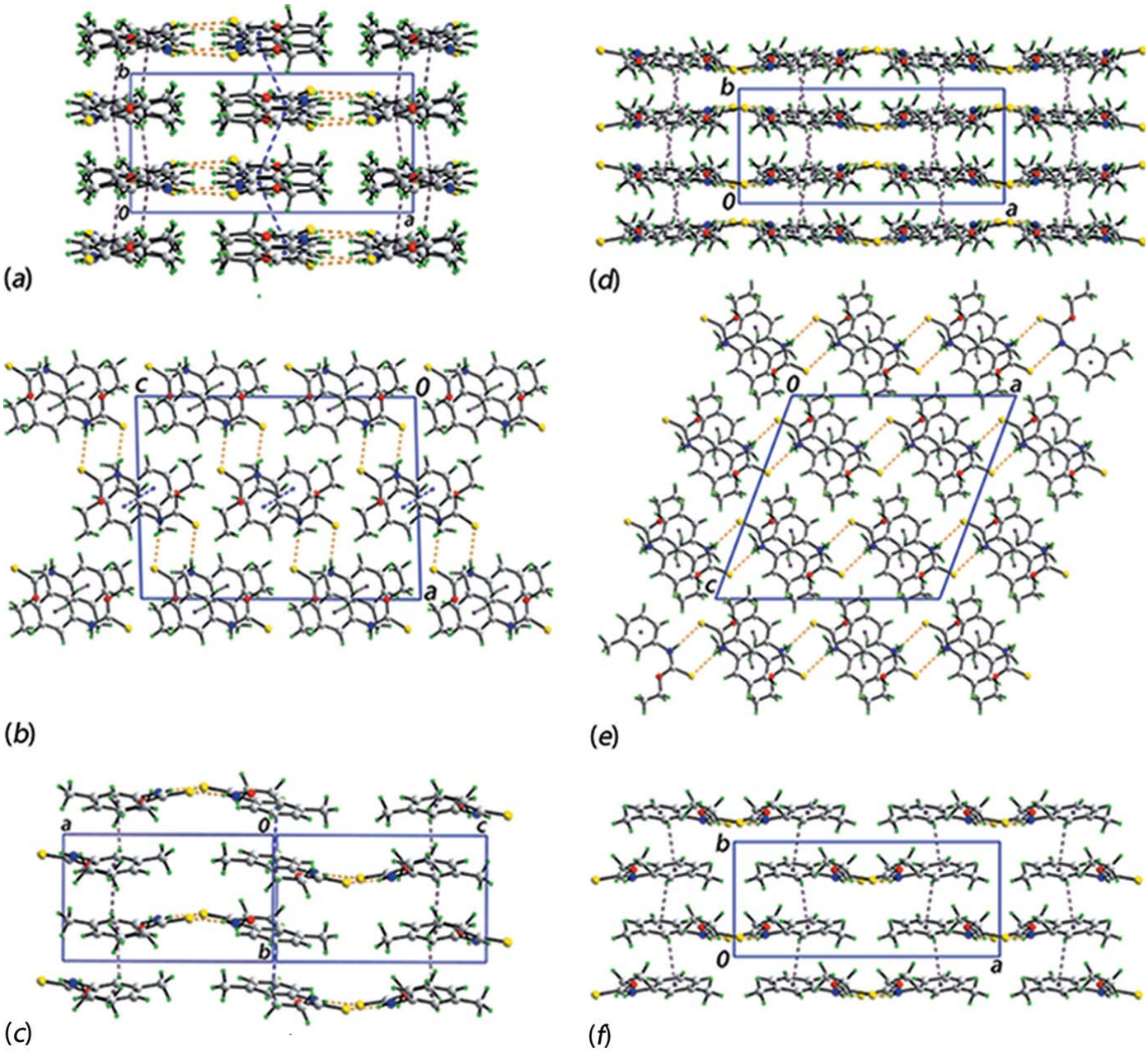

Figure 4
Molecular packing in (Ip): (*a*) a view of the unit-cell contents shown in projection down the *c* axis, (*b*) a view of the unit-cell contents shown in projection down the *b* axis and (*c*) a view of the supramolecular layer. Molecular packing in (Ic): (*d*) a view of the unit-cell contents shown in projection down the *c* axis, (*e*) a view of the unit-cell contents shown in projection down the *b* axis and (*f*) a view of the supramolecular layer. The thioamide-N—H···S(thione), C—H···π and π–π interactions are shown as orange, purple and blue dashed lines, respectively.

the intermolecular interactions instrumental in the crystals of the polymorphs.

The appearance of bright-red spots near the thioamide-H and thione-S atoms, diminutive red spots near the 3-tolyl-H, ethoxy-H atoms and thione-S atoms on the Hirshfeld surfaces mapped over d_{norm} shown in Fig. 5 for both independent molecules of (Ip) as well as for polymorph (Ic) are indicative of comparable thioamide-N—H···S(thione) and 3-tolyl-C—H···S(thione) interactions, and short interatomic H···H contacts in their respective crystals, Table 4; values in Table 4 were obtained from an analysis employing the *CrystalExplorer* package (Wolff *et al.* 2012). As there are two independent molecules in monoclinic polymorph (Ip), it exhibits a pair of the above-mentioned intermolecular interactions shown with labels 1 to 4 in Fig. 5*a*–*c*, whereas in form (Ic) they are labelled as 1 and 2 in Fig. 5*d* and *e*. In addition to the above, the faint-red spots viewed near 3-tolyl-C14 in Fig. 5*b* and ethoxy-H20*B* in Fig. 5*c* indicate the significance of short interatomic C···H/H···C contacts, Table 4, in the packing of (Ip). The donors and acceptors of intermolecular interactions are also represented

Table 4
Summary of short interatomic contacts (Å) in (Ip) and (Ic)[a].

Contact	Distance	Symmetry operation
(Ip)		
H3···H14	2.35	$x, \frac{3}{2}-y, -\frac{1}{2}+z$
H5···H9*B*	2.28	$x, \frac{3}{2}-y, \frac{1}{2}+z$
H15···H19*A*	2.31	$x, \frac{3}{2}-y, -\frac{1}{2}+z$
H19*B*···H19*B*	2.08	$2-x, 2-y, 1-z$
C10···H20*C*	2.87	$-1+x, y, z$
C14···H20*B*	2.77	$2-x, -\frac{1}{2}+y, \frac{1}{2}-z$
N1···H18*B*	2.73	$2-x, -\frac{1}{2}+y, \frac{1}{2}-z$
(Ic)		
H7···H9*b*	2.37	$\frac{1}{2}+x, \frac{1}{2}-y, \frac{1}{2}+z$
H9*a*···H9*a*	2.11	$-x, -y, -z$
H10*b*···H10*b*	2.32	$\frac{1}{2}-x, \frac{1}{2}-y, -z$

Note: (*a*) the atom numbering for the molecule in (Ic) follows that for the S1-molecule in (Ip).

with blue and red regions, respectively, on the Hirshfeld surfaces mapped over electrostatic potential in Fig. 6. The new monoclinic polymorph (Ip) has distinct and a greater number of short interatomic contacts than for (Ic) owing, in part, to the presence of two distinct molecules per asymmetric unit, Table 4. The short interatomic H···H contacts together with intermolecular N—H···S and C—H···S interactions formed with the atoms of reference molecules within Hirshfeld

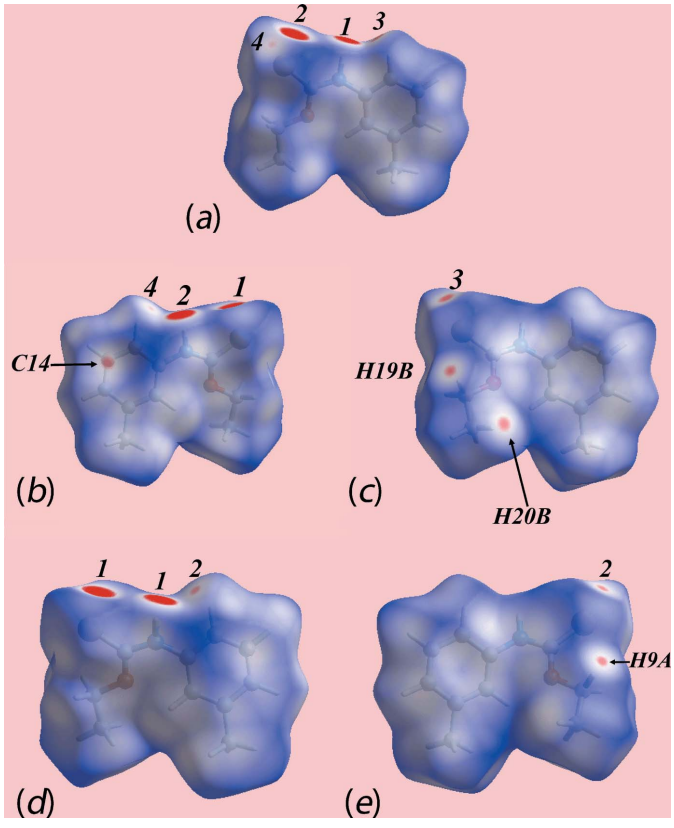

Figure 5
Views of the Hirshfeld surfaces mapped over d_{norm} for the (*a*) S1-containing molecule of (Ip) in the range −0.147 to +1.345 au, (*b*) and (*c*) S11-containing molecule in (Ip) in the range −0.149 to +1.274 au and (*d*) and (*e*) molecule of polymorph (Ic) in the range −0.109 to 1.397 au.

Table 5
Percentage contributions of interatomic contacts to the Hirshfeld surfaces for the individual molecules in (Ip), overall (Ip) and (Ic).

Contact	Percentage contribution			
	(Ip), S1-molecule	(Ip), S11-molecule	overall (Ip)	(Ic)
H···H	57.4	55.5	61.7	57.0
S···H/H···S	17.6	17.4	10.0	17.3
C···H/H···C	14.0	18.8	17.8	17.3
C···C	3.9	1.5	3.0	1.9
N···H/H···N	2.6	2.9	3.0	2.6
C···O/O···C	2.5	2.5	2.7	2.4
O···H/H···O	1.0	1.2	1.2	1.1
C···N/N···C	0.9	0.3	0.6	0.4

surfaces mapped over electrostatic potential for (Ip) and (Ic) are highlighted in Fig. 7.

The overall two-dimensional fingerprint plots for the S1 and S11-containing molecules of (Ip), the whole asymmetric unit of (Ip) and for the polymorph (Ic) are illustrated in Fig. 8*a*–*d*,

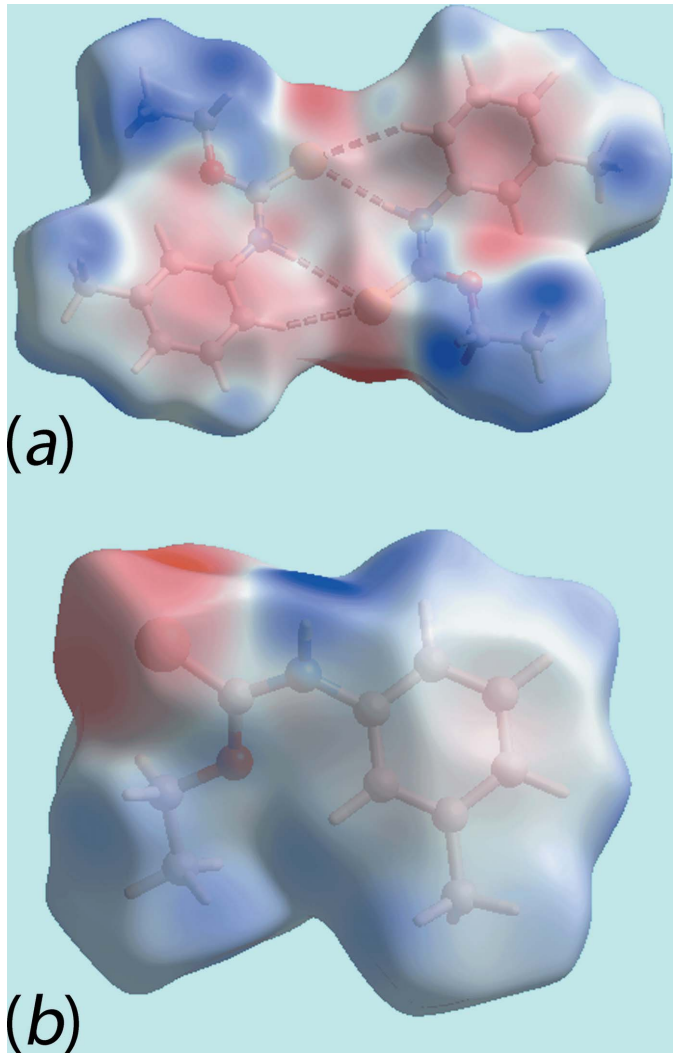

Figure 6
Views of Hirshfeld surfaces mapped over the electrostatic potential for (*a*) the asymmetric unit of (Ip) in the ±0.046 au range and (*b*) molecule of (Ic) in ±0.069 au range. The red and blue regions represent negative and positive electrostatic potentials, respectively.

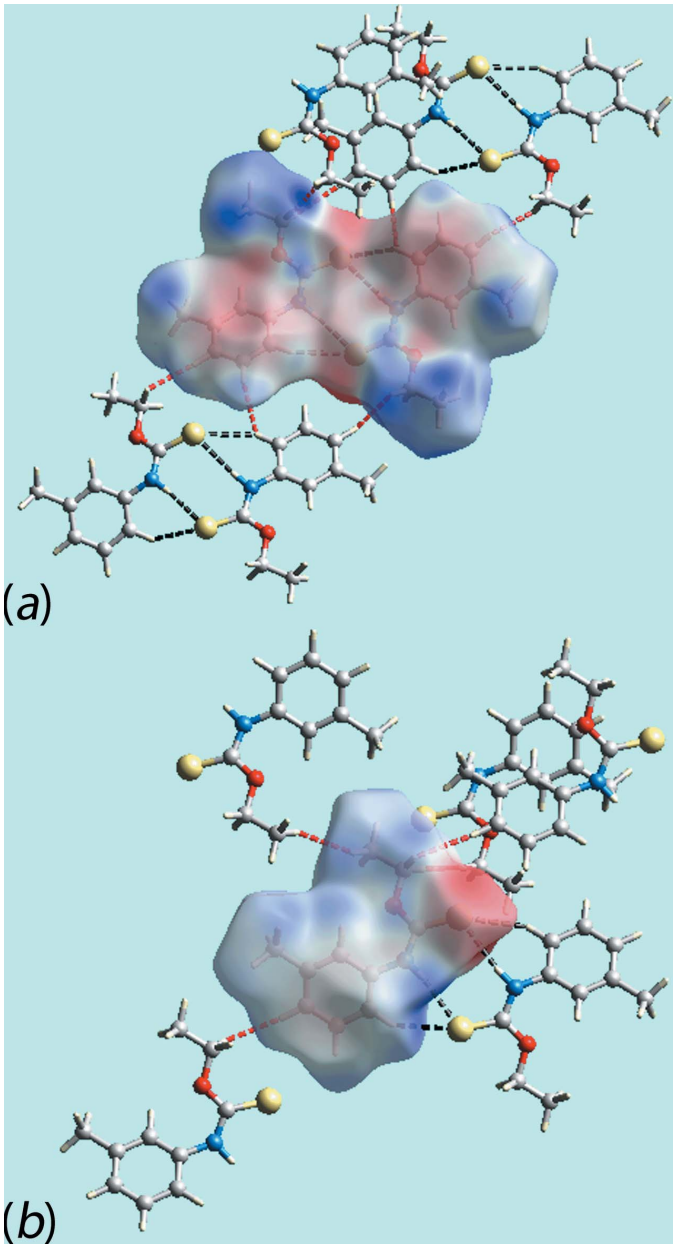

Figure 7
Views of the Hirshfeld surfaces about a reference molecule mapped over the electrostatic potential highlighting the short interatomic H···H contacts (red dashed lines) and intermolecular N—H···S and C—H···S interactions (black dashed lines) in (*a*) (Ip) and (*b*) (Ic).

respectively. In addition, the fingerprint plots delineated into H···H, S···H/H···S, C···H/H···C, C···C and N···H/H···N contacts (McKinnon *et al.*, 2007) are included in Fig. 8; the relative contributions from different interatomic contacts to the Hirshfeld surfaces are summarized in Table 5. The nearly similar distribution of points in the fingerprint plots for S11-containing molecule of (Ip) and that of (Ic) indicate similarity in their molecular environments although some of the equivalent interatomic distances differ, Tables 2–4.

The fingerprint plots delineated into H···H contacts, Fig. 8*b* and *d*, have needle-like tips pointing at $d_e + d_i \sim 2.1$ Å indicating short interatomic H···H contacts, Table 4, for the S11-containing molecule of (Ip) and for (Ic), both involving ethoxy-H atoms. The other short interatomic contacts in both forms are characterized from the points located within the pair of short peaks in (Ip) and a single short peak in (Ic), respectively, at $d_e + d_i < 2.4$ Å, *i.e.* at the sum of their van der Waals radii.

The involvement of ethoxy-H atoms in short interatomic C···H/H···C contacts decreases the percentage contribution from H···H contacts to the Hirshfeld surface of the S11-containing molecule whereas the contribution from equivalent contacts to the surface of the S1-containing molecule of (Ip) and that of (Ic) are almost same, Table 5. The increase in percentage contribution from these contacts to the Hirshfeld surface of overall asymmetric unit of (Ip) is due to the intermolecular N—H···S and C—H···S interactions between the respective atoms of S1- and S11-containing molecules thereby decreasing the contribution from S···H/H···S contacts to the overall surface, Table 5. This fact is confirmed from the nearly same percentage contribution from S···H/H···S contacts to the Hirshfeld surfaces of the individual S1- and S11-containing molecules of (Ip) and of the molecule of the (Ic) form, Table 5, and also from pair of forceps-like tips at $d_e + d_i \sim 2.6$ Å with the nearly same distribution of points in their respective fingerprint plots in Fig. 8.

The similar distribution of points in the fingerprint plot delineated into C···H/H···C contacts for the S11-containing molecule of (Ip), Fig. 8*b*, and of (Ic), Fig. 8*d*, indicate their involvement in the intermolecular C—H···π contacts showing pairs of tips at $d_e + d_i \sim 2.8$ and 2.9 Å, respectively. This is confirmed by the slight increase in the percentage contribution from these contacts to the Hirshfeld surface of the S11-containing molecule of (Ip) *cf.* the S1-containing molecule, Table 5. In other words, the contribution from C···H/H···C contacts to the surface of the S1-containing molecule of (Ip), Table 5, is decreased due to the absence of C—H···π contacts involving this molecule whereas the greater percentage contribution from C···C contacts to the Hirshfeld surface of this molecule results from the presence of π–π stacking interactions between the symmetry-related 3-tolyl rings. This is also evident from the arrow-like distribution of points around $d_e = d_i = 1.8$ Å in the C···C delineated fingerprint plot shown in Fig. 8*a*.

The contribution of 3.0% from N···H/H···N contacts to the Hirshfeld surface of whole asymmetric unit of polymorph (Ip) indicate the presence of short interatomic N···H/H···N contacts between the thioamide-N1 and tolyl-H18*B* atoms, Table 4, although all of the delineated fingerprint plots have a similar distributions of points, Fig. 8, at least to a first approximation. The other interatomic contacts summarized in Table 4 make only small contributions to the Hirshfeld surfaces and have negligible contributions on the respective molecular packings.

5. Database survey

According to a search of the Cambridge Structural Database (Version 5.38, May update; Groom *et al.*, 2016), there are 22

Table 6
Hydrogen-bonding patterns in *R*OC(=S)N(H)*R*′.

Number	*R*	*R*′	*Z*′	Hydrogen bonds	Motif	Refcode	Ref.
(II)	Me	phenyl	1	N—H···S	**A**	OJIHAQ	Ho *et al.* (2003)
(III)	Me	4-NO_2-phenyl	1	N—H···S	**A**	CAZFUF	Ho *et al.* (2005)
(IV)	Me	4-*C*(=O)OMe-phenyl	1	N—H···S	**A**	CAZGAM	Ho *et al.* (2005)
(V)	Me	4-Cl-phenyl	2	N—H···S	**A**′	CAZCEQ	Ho *et al.* (2005)
(VI)	Me	4-*C*(=O)Me-phenyl	1	N—H···O	**B**	CAZGIU	Ho *et al.* (2005)
(VII)	Me	2-tolyl	1	N—H···S	**A**	TAZSIX	Kuan *et al.* (2005)
(VIII)	Me	4-tolyl	2	N—H···S	**A**′	TIBYUZ	Ho *et al.* (2007)
(IX)	Et	phenyl	3	N—H···S	**A**″	PINPIL	Taylor & Tiekink (1994)
(Ip)	Et	3-tolyl	2	N—H···S	**A**′	–	This work
(Ip)	Et	3-tolyl	1	N—H···S	**A**‴	TAZTUK	Tadbuppa & Tiekink (2005)
(*X*)	Et	4-tolyl	1	N—H···S	**A**	TIBYOT	Tadbuppa & Tiekink (2007*a*)
(XI)	Et	3-OMe-phenyl	1	N—H···S	**A**	UDUPAL	Hanif *et al.* (2007)
(XII)	Et	4-NO_2-phenyl	1	N—H···S	**A**	NENLAU	Benson *et al.* (2006)
(XIII)	Et	4-Cl-phenyl	1	N—H···S	**A**	DEYQEE	Tadbuppa & Tiekink (2007*b*)
(XIV)	*n*-Pr	phenyl	2	N—H···S	**A**′	PAWKAB	Sudkaow *et al.* (2012)
(XV)	*i*-Pr	Ph	1	N—H···S	**A**	ADOGUW	Kuan *et al.* (2007)
(XVI)	*i*-Pr	4-tolyl	1	N—H···S	**A**	ADOGOQ	Kuan *et al.* (2007)
(XVII)	*i*-Pr	4-Cl-phenyl	1	N—H···S	**A**	ADOHAD	Kuan *et al.* (2007)
(XVIII)	*i*-Pr	4-NO_2-phenyl	1	N—H···S	**A**	MISDEY	Ellis *et al.* (2008)
(XIX)	4-pyridylmethyl	phenyl	2	N—H···N	**C**	IFACOI	Xiao *et al.* (2006)
(XX)	*i*-Bu	phenyl	1	N—H···S	**A**‴	KEQJAS	Jian *et al.* (2006)
(XXI)	2,4-Me_2-phenyl	phenyl	1	N—H···S	**A**	POVVOL	Abraham *et al.* (1995)
(XXII)	2,4-$(OMe)_2$-phenyl	R^{1a}	1	N—H···N	**C**	OSIZOG	Zhou *et al.* (2010)
(XXIII)	Cy	phenyl	2	N—H···S	**A**′	VEFKUO	Sahoo *et al.* (2012)

Note: (*a*) see Scheme 2 for the chemical diagram of (XXII).

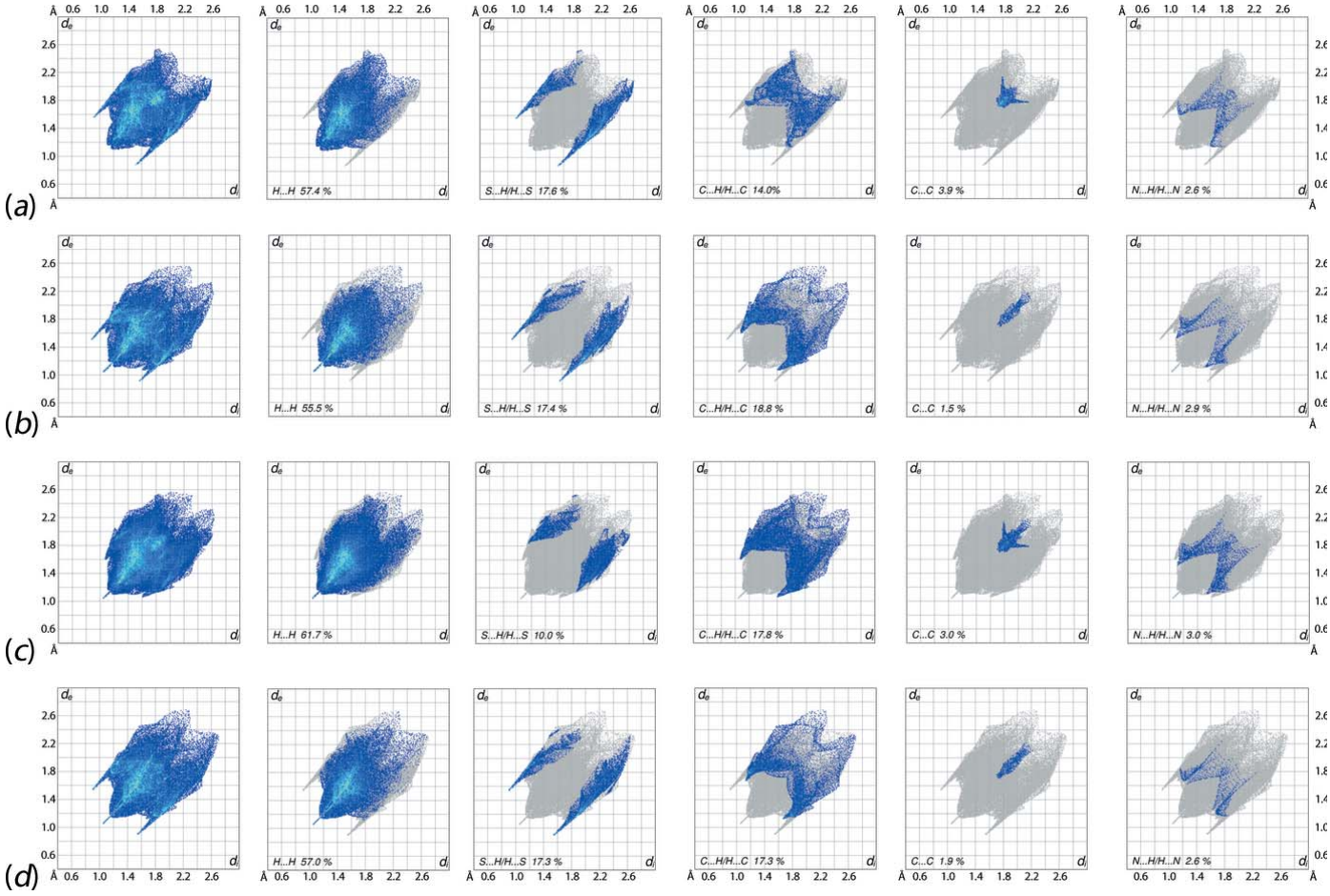

Figure 8
The full two-dimensional fingerprint plot and those delineated into H···H, S···H/H···S, C···H/H···C, C···C and N···H/H···N (left to right) contacts for (*a*) S1-molecule of (Ip), (*b*) S11-molecule of (Ip), (*c*) overall (Ip) and (*d*) (Ic).

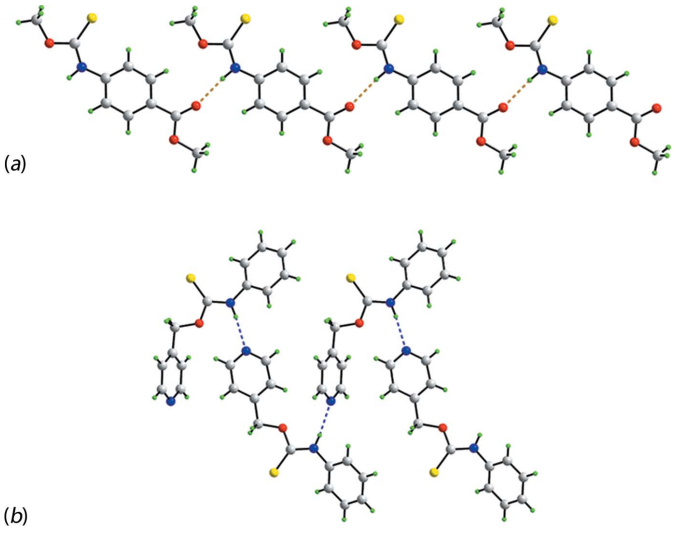

Figure 9
Supramolecular aggregation in related carbothioamide structures: (*a*) linear supramolecular chain in the crystal of MeOC(═S)N(H)(4-C(═O)Me-phenyl) (VI) mediated by thioamide-N—H···O(carboxy) hydrogen bonding shown as orange dashed lines and (*b*) zigzag chain in the crystal of (4-pyridyl)CH_2OC(═S)N(H)phenyl mediated by thioamide-N—H···N(pyridyl) hydrogen bonding shown as blue dashed lines.

monofunctional carbothioamide molecules related to the title compound, with (Ip) and (Ic) being the only pair of polymorphs characterized thus far. Referring to Table 6, the overwhelming majority of the 24 crystallographically characterized thioamides feature an eight-membered thioamide, $\{\cdots SCNH\}_2$, synthon. Thus, in 13 of the characterized structures, the synthon is formed about a centre of inversion, motif **A**. In five structures, two independent molecules (Z' = 2) comprise the asymmetric unit, as in (Ip), and these associated *via* the $\{\cdots SCNH\}_2$ synthon but with no crystallographically imposed symmetry, motif **A′**. There is a single example of a structure with Z' = 3 (Taylor & Tiekink, 1994). Here, one of the independent molecules self-associates about a centre of inversion, as in motif **A**, whereas the two remaining independent molecules are connected by the $\{\cdots SCNH\}_2$ synthon, as found in motif **A′**. This is motif **A″**. Two structures feature the $\{\cdots SCNH\}_2$ synthon located about a twofold axis of symmetry, as in (Ic), *i.e.* motif **A‴**. The remaining three structures do not feature thioamide-N—H···S(thione) hydrogen bonding. In the structure of MeOC(═S)N(H)(4-C(═O)Me-phenyl) (VI) (Ho *et al.*, 2005), motif **B**, thioamide-N—H···O(carboxy) hydrogen bonding is observed, leading to a linear supramolecular chain as shown in Fig. 9*a*. This structure is noteworthy as being the only example where the conformation of the thioamide moiety is *anti* rather than the normally observed *syn*. The final variation, motif **C**, is found in two structures, Table 6. The structure of (4-pyridyl)-CH_2OC(═S)N(H)phenyl (XIX) (Xiao *et al.*, 2006) serves as an exemplar. Thus, in the crystal of (XIX), thioamide-N—H···N(pyridyl) hydrogen bonds lead to a zigzag chain as shown in Fig. 9*b*. In summary, an inspection of the data in Table 6 indicates the predominance of thioamide-N—H···S(thione) hydrogen bonding in these carbothioamides, at least in the absence of competing synthons, as seen in motifs **B** and **C**

Table 7
Experimental details.

Crystal data	
Chemical formula	$C_{10}H_{13}NOS$
M_r	195.27
Crystal system, space group	Monoclinic, $P2_1/c$
Temperature (K)	100
a, b, c (Å)	14.3999 (5), 7.0388 (3), 19.9725 (7)
β (°)	91.727 (3)
V (Å^3)	2023.45 (13)
Z	8
Radiation type	Mo $K\alpha$
μ (mm^{-1})	0.28
Crystal size (mm)	0.20 × 0.20 × 0.05
Data collection	
Diffractometer	Agilent SuperNova, Dual, Mo at zero, Atlas
Absorption correction	Multi-scan (*CrysAlis PRO*; Agilent, 2011)
T_{min}, T_{max}	0.662, 1.000
No. of measured, independent and observed [$I > 2\sigma(I)$] reflections	15588, 4577, 3514
R_{int}	0.040
(sin $\theta/\lambda)_{max}$ (Å^{-1})	0.651
Refinement	
$R[F^2 > 2\sigma(F^2)]$, $wR(F^2)$, S	0.047, 0.125, 1.03
No. of reflections	4577
No. of parameters	245
No. of restraints	2
H-atom treatment	H atoms treated by a mixture of independent and constrained refinement
$\Delta\rho_{max}$, $\Delta\rho_{min}$ (e Å^{-3})	0.72, −0.24

Computer programs: *CrysAlis PRO* (Agilent, 2011), *SHELXS97* (Sheldrick, 2008), *SHELXL2014* (Sheldrick, 2015), *ORTEP-3 for Windows* (Farrugia, 2012), *QMol* (Gans & Shalloway, 2001), *DIAMOND* (Brandenburg, 2006) and *publCIF* (Westrip, 2010).

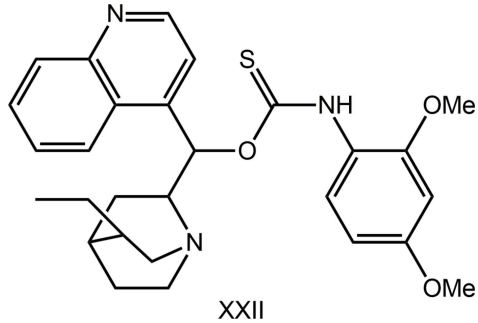

XXII

6. Synthesis and crystallization

All chemicals and solvents were used as purchased without purification. To prepare (Ip), 3-tolyl isothiocyanate (Merck; 2.5 mmol, 0.34 ml) was added to NaOH (Merck; 2.5 mmol, 0.10 g) in EtOH (Merck; 3 ml) and the mixture was stirred at room temperature for 2 h, followed by the addition of excess 5 *M* HCl solution. The resulting mixture was stirred for another 1.5 h. The final product was extracted with chloroform (Merck; 10 ml) and left for evaporation at room temperature,

yielding brown crystals after 1 week. M.p. (Krüss KSP1N melting point meter): 339–340 K. IR (Perkin Elmer Spectrum 400 FT Mid-IR/Far-IR spectrophotometer; cm^{-1}): 3211 (*s*) (N—H), 1451 (*s*) (C—N), 1209 (*s*) (C═S), 1064 (*s*) (C—O).

7. Refinement

Crystal data, data collection and structure refinement details are summarized in Table 7. The carbon-bound H atoms were placed in calculated positions (C—H = 0.95–0.99 Å) and were included in the refinement in the riding-model approximation, with U_{iso}(H) set to 1.2–1.5U_{eq}(C). The nitrogen-bound H atoms were located in a difference Fourier map but were refined with a distance restraint of N—H = 0.88±0.01 Å, and with U_{iso}(H) set to 1.2U_{eq}(N). Owing to poor agreement, one reflection, *i.e.* ($\overline{1}5$ 1 4), was omitted from the final cycles of refinement.

Acknowledgements

The authors thank the staff of the University of Malaya's X-ray diffraction laboratory for the data collection. Sunway University is thanked for support of biological and crystal engineering studies of carbothioamides and their coinage metal complexes.

References

Abraham, S. P., Samuelson, A. G. & Nethaji, M. (1995). *Proc. Indian Acad. Sci. Chem. Sci.* **107**, 255–271.
Agilent (2011). *CrysAlis PRO*. Agilent Technologies, Yarnton, England.
Benson, R. E., Broker, G. A., Daniels, L. M., Tiekink, E. R. T., Wardell, J. L. & Young, D. J. (2006). *Acta Cryst.* E**62**, o4106–o4108.
Brandenburg, K. (2006). *DIAMOND*. Crystal Impact GbR, Bonn, Germany.
Ellis, C. A., Miller, M. A., Spencer, J., Zukerman-Schpector, J. & Tiekink, E. R. T. (2009). *CrystEngComm*, **11**, 1352–1361.
Ellis, C. A., Tiekink, E. R. T. & Zukerman-Schpector, J. (2008). *Acta Cryst.* E**64**, o345.
Farrugia, L. J. (2012). *J. Appl. Cryst.* **45**, 849–854.
Gans, J. & Shalloway, D. (2001). *J. Mol. Graph. Model.* **19**, 557–609.
Groom, C. R., Bruno, I. J., Lightfoot, M. P. & Ward, S. C. (2016). *Acta Cryst.* B**72**, 171–179.
Hanif, M., Qadeer, G., Shi, L. & Rama, N. H. (2007). *Acta Cryst.* E**63**, o3062.
Ho, S. Y., Bettens, R. P. A., Dakternieks, D., Duthie, A. & Tiekink, E. R. T. (2005). *CrystEngComm*, **7**, 682–689.
Ho, S. Y., Cheng, E. C.-C., Tiekink, E. R. T. & Yam, V. W.-W. (2006). *Inorg. Chem.* **45**, 8165–8174.
Ho, S. Y., Kuan, F. S. & Tiekink, E. R. T. (2007). *Acta Cryst.* E**63**, o1723–o1724.
Ho, S. Y., Lai, C. S. & Tiekink, E. R. T. (2003). *Acta Cryst.* E**59**, o1155–o1156.
Jian, F.-F., Yu, H.-Q., Qiao, Y.-B. & Liang, T.-L. (2006). *Acta Cryst.* E**62**, o3416–o3417.
Kuan, F. S., Jotani, M. M. & Tiekink, E. R. T. (2017). *Acta Cryst.* E**73**, 1465–1471.
Kuan, F. S., Mohr, F., Tadbuppa, P. P. & Tiekink, E. R. T. (2007). *CrystEngComm*, **9**, 574–581.
Kuan, F. S., Tadbuppa, P. P. & Tiekink, E. R. T. (2005). *Z. Kristallogr. New Cryst. Struct.* **220**, 393–394.
McKinnon, J. J., Jayatilaka, D. & Spackman, M. A. (2007). *Chem. Commun.* pp. 3814–3816.
Ooi, K. K., Yeo, C. I., Mahandaran, T., Ang, K. P., Akim, A. M., Cheah, Y.-K., Seng, H.-L. & Tiekink, E. R. T. (2017). *J. Inorg. Biochem.* **166**, 173–181.
Sahoo, S. K., Chakraborty, S. & Patel, B. K. (2012). *J. Sulfur Chem.* **33**, 143–153.
Sheldrick, G. M. (2008). *Acta Cryst.* A**64**, 112–122.
Sheldrick, G. M. (2015). *Acta Cryst.* C**71**, 3–8.
Slater, N. H., Buckley, B. R., Elsegood, M. R. J., Teat, S. J. & Kimber, M. C. (2016). *Cryst. Growth Des.* **16**, 3846–3852.
Spek, A. L. (2009). *Acta Cryst.* D**65**, 148–155.
Sudkaow, P., Yeo, C. I., Ng, S. W. & Tiekink, E. R. T. (2012). *Acta Cryst.* E**68**, o1774.
Tadbuppa, P. P. & Tiekink, E. R. T. (2005). *Z. Kristallogr. New Cryst. Struct.* **220**, 395–396.
Tadbuppa, P. P. & Tiekink, E. R. T. (2007*a*). *Acta Cryst.* E**63**, o1779–o1780.
Tadbuppa, P. P. & Tiekink, E. R. T. (2007*b*). *Acta Cryst.* E**63**, o1885–o1886.
Taylor, R. L. & Tiekink, E. R. T. (1994). *Z. Kristallogr.* **209**, 64–67.
Westrip, S. P. (2010). *J. Appl. Cryst.* **43**, 920–925.
Wolff, S. K., Grimwood, D. J., McKinnon, J. J., Turner, M. J., Jayatilaka, D. & Spackman, M. A. (2012). University of Western Australia.
Xiao, H.-L., Wang, K.-F. & Jian, F.-F. (2006). *Acta Cryst.* E**62**, o2852–o2853.
Yeo, C. I., Halim, S. N. A., Ng, S. W., Tan, S. L., Zukerman-Schpector, J., Ferreira, M. A. B. & Tiekink, E. R. T. (2014). *Chem. Commun.* **50**, 5984–5986.
Yeo, C. I., Sim, J.-H., Khoo, C.-H., Goh, Z.-J., Ang, K.-P., Cheah, Y.-K., Fairuz, Z. A., Halim, S. N. B. A., Ng, S. W., Seng, H.-L. & Tiekink, E. R. T. (2013). *Gold Bull.* **46**, 145–152.
Zhou, L., Tan, C. K., Jiang, X., Chen, F. & Yeung, Y.-Y. (2010). *J. Am. Chem. Soc.* **132**, 15474–15476.
Zukerman-Schpector, J., Yeo, C. I. & Tiekink, E. R. T. (2016). *Z. Kristallogr.* **231**, 55–64.

supporting information

Acta Cryst. (2017). E**73**, 1889-1897 [https://doi.org/10.1107/S2056989017016280]

A new monoclinic polymorph of *N*-(3-methylphenyl)ethoxycarbothioamide: crystal structure and Hirshfeld surface analysis

Mukesh M. Jotani, Chien Ing Yeo and Edward R. T. Tiekink

Computing details

Data collection: *CrysAlis PRO* (Agilent, 2011); cell refinement: *CrysAlis PRO* (Agilent, 2011); data reduction: *CrysAlis PRO* (Agilent, 2011); program(s) used to solve structure: *SHELXS97* (Sheldrick, 2008); program(s) used to refine structure: *SHELXL2014* (Sheldrick, 2015); molecular graphics: *ORTEP-3 for Windows* (Farrugia, 2012), *QMol* (Gans & Shalloway, 2001) and *DIAMOND* (Brandenburg, 2006); software used to prepare material for publication: *publCIF* (Westrip, 2010).

N-(3-Methylphenyl)ethoxycarbothioamide

Crystal data

$C_{10}H_{13}NOS$
M_r = 195.27
Monoclinic, $P2_1/c$
a = 14.3999 (5) Å
b = 7.0388 (3) Å
c = 19.9725 (7) Å
β = 91.727 (3)°
V = 2023.45 (13) Å^3
Z = 8
$F(000)$ = 832
D_x = 1.282 Mg m^{-3}
Mo $K\alpha$ radiation, λ = 0.71073 Å
Cell parameters from 6144 reflections
θ = 2.4–27.5°
μ = 0.28 mm^{-1}
T = 100 K
Slab, colourless
0.20 × 0.20 × 0.05 mm

Data collection

Agilent SuperNova, Dual, Mo at zero, Atlas diffractometer
Radiation source: SuperNova (Mo) X-ray Source
Mirror monochromator
Detector resolution: 10.4041 pixels mm^{-1}
ω scan
Absorption correction: multi-scan (CrysAlis PRO; Agilent, 2011)
T_{min} = 0.662, T_{max} = 1.000
15588 measured reflections
4577 independent reflections
3514 reflections with $I > 2\sigma(I)$
R_{int} = 0.040
θ_{max} = 27.6°, θ_{min} = 2.5°
h = −18→18
k = −9→9
l = −18→25

Refinement

Refinement on F^2
Least-squares matrix: full
$R[F^2 > 2\sigma(F^2)]$ = 0.047
$wR(F^2)$ = 0.125
S = 1.03
4577 reflections
245 parameters
2 restraints
H atoms treated by a mixture of independent and constrained refinement
$w = 1/[\sigma^2(F_o^2) + (0.0629P)^2 + 0.8006P]$ where $P = (F_o^2 + 2F_c^2)/3$
$(\Delta/\sigma)_{max}$ = 0.001
$\Delta\rho_{max}$ = 0.72 e Å^{-3}
$\Delta\rho_{min}$ = −0.24 e Å^{-3}

Special details

Geometry. All esds (except the esd in the dihedral angle between two l.s. planes) are estimated using the full covariance matrix. The cell esds are taken into account individually in the estimation of esds in distances, angles and torsion angles; correlations between esds in cell parameters are only used when they are defined by crystal symmetry. An approximate (isotropic) treatment of cell esds is used for estimating esds involving l.s. planes.

Fractional atomic coordinates and isotropic or equivalent isotropic displacement parameters (Å²)

	x	*y*	*z*	U_{iso}*/U_{eq}
S1	0.63595 (3)	0.62560 (8)	0.29847 (2)	0.02560 (15)
O1	0.48087 (9)	0.6728 (2)	0.36508 (7)	0.0205 (3)
N1	0.61175 (11)	0.6959 (2)	0.42674 (8)	0.0176 (3)
H1N	0.6720 (7)	0.683 (3)	0.4295 (11)	0.021*
C1	0.57256 (13)	0.6663 (3)	0.36605 (10)	0.0183 (4)
C2	0.57411 (12)	0.7410 (3)	0.48972 (9)	0.0157 (4)
C3	0.63901 (13)	0.7851 (3)	0.54059 (10)	0.0198 (4)
H3	0.7035	0.7828	0.5318	0.024*
C4	0.60988 (14)	0.8320 (3)	0.60359 (10)	0.0224 (4)
H4	0.6545	0.8604	0.6382	0.027*
C5	0.51590 (14)	0.8380 (3)	0.61691 (10)	0.0214 (4)
H5	0.4963	0.8719	0.6603	0.026*
C6	0.45044 (13)	0.7944 (3)	0.56662 (10)	0.0189 (4)
C7	0.47948 (13)	0.7455 (3)	0.50316 (10)	0.0185 (4)
H7	0.4349	0.7151	0.4688	0.022*
C8	0.34802 (13)	0.8043 (3)	0.58036 (11)	0.0258 (5)
H8A	0.3157	0.6989	0.5576	0.039*
H8B	0.3227	0.9252	0.5637	0.039*
H8C	0.3391	0.7952	0.6287	0.039*
C9	0.43042 (14)	0.6465 (3)	0.30146 (10)	0.0250 (5)
H9A	0.4433	0.5193	0.2827	0.030*
H9B	0.4489	0.7440	0.2687	0.030*
C10	0.33069 (15)	0.6655 (4)	0.31611 (12)	0.0334 (5)
H10A	0.2934	0.6493	0.2747	0.050*
H10B	0.3192	0.7917	0.3349	0.050*
H10C	0.3135	0.5680	0.3485	0.050*
S11	0.85195 (3)	0.66025 (9)	0.45041 (2)	0.02577 (15)
O11	0.99877 (9)	0.7448 (2)	0.37829 (6)	0.0192 (3)
N11	0.86976 (10)	0.6753 (2)	0.31952 (8)	0.0175 (3)
H11N	0.8103 (7)	0.652 (3)	0.3174 (11)	0.021*
C11	0.91055 (13)	0.6951 (3)	0.38026 (10)	0.0185 (4)
C12	0.90609 (12)	0.7096 (3)	0.25516 (9)	0.0156 (4)
C13	0.84323 (12)	0.7751 (3)	0.20604 (9)	0.0179 (4)
H13	0.7802	0.7967	0.2165	0.021*
C14	0.87304 (13)	0.8082 (3)	0.14206 (9)	0.0193 (4)
H14	0.8303	0.8523	0.1084	0.023*
C15	0.96520 (13)	0.7774 (3)	0.12656 (9)	0.0192 (4)
H15	0.9854	0.8019	0.0825	0.023*
C16	1.02797 (13)	0.7108 (3)	0.17527 (10)	0.0177 (4)

C17	0.99808 (13)	0.6749 (3)	0.23923 (9)	0.0176 (4)
H17	1.0404	0.6265	0.2724	0.021*
C18	1.12821 (13)	0.6769 (3)	0.15808 (10)	0.0245 (5)
H18A	1.1566	0.5877	0.1904	0.037*
H18B	1.1622	0.7975	0.1599	0.037*
H18C	1.1308	0.6234	0.1129	0.037*
C19	1.05091 (14)	0.7744 (3)	0.44091 (10)	0.0256 (5)
H19A	1.0493	0.6584	0.4689	0.031*
H19B	1.0238	0.8806	0.4663	0.031*
C20	1.14753 (15)	0.8193 (4)	0.42346 (12)	0.0349 (5)
H20A	1.1840	0.8490	0.4643	0.052*
H20B	1.1477	0.9291	0.3933	0.052*
H20C	1.1750	0.7096	0.4012	0.052*

Atomic displacement parameters (Å²)

	U^{11}	U^{22}	U^{33}	U^{12}	U^{13}	U^{23}
S1	0.0230 (3)	0.0401 (3)	0.0140 (3)	−0.0017 (2)	0.00422 (18)	−0.0020 (2)
O1	0.0190 (7)	0.0284 (8)	0.0141 (7)	0.0011 (6)	−0.0009 (5)	−0.0020 (6)
N1	0.0155 (7)	0.0236 (9)	0.0139 (8)	0.0005 (7)	0.0022 (6)	−0.0005 (7)
C1	0.0200 (9)	0.0174 (10)	0.0176 (10)	−0.0011 (8)	0.0017 (7)	0.0017 (8)
C2	0.0211 (9)	0.0129 (9)	0.0132 (9)	0.0008 (7)	0.0039 (7)	0.0011 (7)
C3	0.0182 (9)	0.0233 (11)	0.0178 (10)	0.0014 (8)	0.0019 (7)	0.0004 (8)
C4	0.0251 (10)	0.0262 (11)	0.0157 (10)	−0.0002 (9)	−0.0014 (8)	−0.0010 (8)
C5	0.0279 (10)	0.0234 (11)	0.0133 (9)	0.0026 (8)	0.0052 (7)	−0.0009 (8)
C6	0.0205 (9)	0.0181 (10)	0.0184 (10)	−0.0003 (8)	0.0052 (7)	0.0035 (8)
C7	0.0199 (9)	0.0203 (10)	0.0154 (10)	−0.0016 (8)	0.0014 (7)	0.0020 (8)
C8	0.0226 (10)	0.0331 (12)	0.0221 (11)	0.0014 (9)	0.0077 (8)	0.0024 (9)
C9	0.0254 (10)	0.0337 (12)	0.0155 (10)	−0.0020 (9)	−0.0057 (8)	−0.0002 (9)
C10	0.0267 (11)	0.0404 (14)	0.0329 (13)	−0.0041 (10)	−0.0037 (9)	−0.0003 (11)
S11	0.0225 (3)	0.0423 (3)	0.0127 (3)	0.0072 (2)	0.00474 (18)	0.0035 (2)
O11	0.0203 (7)	0.0236 (8)	0.0137 (7)	0.0012 (6)	−0.0003 (5)	−0.0007 (6)
N11	0.0147 (7)	0.0238 (9)	0.0141 (8)	0.0025 (7)	0.0027 (6)	0.0016 (7)
C11	0.0200 (9)	0.0200 (10)	0.0155 (9)	0.0075 (8)	0.0027 (7)	0.0009 (8)
C12	0.0196 (9)	0.0152 (9)	0.0121 (9)	−0.0005 (7)	0.0031 (7)	0.0003 (7)
C13	0.0154 (9)	0.0225 (10)	0.0158 (10)	−0.0017 (8)	0.0006 (7)	−0.0010 (8)
C14	0.0219 (9)	0.0217 (10)	0.0141 (9)	−0.0031 (8)	−0.0032 (7)	0.0010 (8)
C15	0.0242 (10)	0.0225 (10)	0.0110 (9)	−0.0033 (8)	0.0030 (7)	0.0001 (8)
C16	0.0198 (9)	0.0161 (9)	0.0175 (10)	−0.0014 (8)	0.0042 (7)	−0.0007 (8)
C17	0.0201 (9)	0.0165 (9)	0.0162 (10)	0.0029 (8)	0.0010 (7)	0.0010 (8)
C18	0.0236 (10)	0.0286 (12)	0.0217 (11)	0.0038 (9)	0.0090 (8)	0.0029 (9)
C19	0.0265 (10)	0.0323 (12)	0.0176 (10)	0.0042 (9)	−0.0044 (8)	−0.0055 (9)
C20	0.0302 (12)	0.0359 (14)	0.0382 (14)	−0.0012 (10)	−0.0047 (10)	−0.0008 (11)

Geometric parameters (Å, º)

S1—C1	1.6768 (19)	S11—C11	1.6752 (19)
O1—C1	1.321 (2)	O11—C11	1.319 (2)

O1—C9	1.457 (2)	O11—C19	1.454 (2)
N1—C1	1.338 (2)	N11—C11	1.339 (2)
N1—C2	1.421 (2)	N11—C12	1.423 (2)
N1—H1N	0.872 (9)	N11—H11N	0.872 (9)
C2—C3	1.394 (3)	C12—C13	1.393 (3)
C2—C7	1.397 (2)	C12—C17	1.393 (2)
C3—C4	1.378 (3)	C13—C14	1.380 (3)
C3—H3	0.9500	C13—H13	0.9500
C4—C5	1.388 (3)	C14—C15	1.389 (3)
C4—H4	0.9500	C14—H14	0.9500
C5—C6	1.391 (3)	C15—C16	1.389 (3)
C5—H5	0.9500	C15—H15	0.9500
C6—C7	1.390 (3)	C16—C17	1.383 (3)
C6—C8	1.510 (3)	C16—C18	1.513 (2)
C7—H7	0.9500	C17—H17	0.9500
C8—H8A	0.9800	C18—H18A	0.9800
C8—H8B	0.9800	C18—H18B	0.9800
C8—H8C	0.9800	C18—H18C	0.9800
C9—C10	1.480 (3)	C19—C20	1.479 (3)
C9—H9A	0.9900	C19—H19A	0.9900
C9—H9B	0.9900	C19—H19B	0.9900
C10—H10A	0.9800	C20—H20A	0.9800
C10—H10B	0.9800	C20—H20B	0.9800
C10—H10C	0.9800	C20—H20C	0.9800

C1—O1—C9	118.72 (15)	C11—O11—C19	119.01 (15)
C1—N1—C2	132.48 (16)	C11—N11—C12	129.60 (16)
C1—N1—H1N	115.6 (15)	C11—N11—H11N	117.9 (15)
C2—N1—H1N	111.9 (15)	C12—N11—H11N	112.0 (15)
O1—C1—N1	113.71 (16)	O11—C11—N11	113.39 (16)
O1—C1—S1	124.23 (14)	O11—C11—S11	125.00 (15)
N1—C1—S1	122.06 (14)	N11—C11—S11	121.61 (15)
C3—C2—C7	119.42 (17)	C13—C12—C17	119.95 (17)
C3—C2—N1	115.45 (16)	C13—C12—N11	116.33 (16)
C7—C2—N1	125.13 (17)	C17—C12—N11	123.68 (17)
C4—C3—C2	120.17 (17)	C14—C13—C12	119.62 (17)
C4—C3—H3	119.9	C14—C13—H13	120.2
C2—C3—H3	119.9	C12—C13—H13	120.2
C3—C4—C5	120.51 (18)	C13—C14—C15	120.40 (17)
C3—C4—H4	119.7	C13—C14—H14	119.8
C5—C4—H4	119.7	C15—C14—H14	119.8
C4—C5—C6	119.90 (18)	C14—C15—C16	120.16 (17)
C4—C5—H5	120.0	C14—C15—H15	119.9
C6—C5—H5	120.0	C16—C15—H15	119.9
C7—C6—C5	119.81 (17)	C17—C16—C15	119.61 (17)
C7—C6—C8	119.97 (18)	C17—C16—C18	120.42 (18)
C5—C6—C8	120.21 (17)	C15—C16—C18	119.96 (17)
C6—C7—C2	120.18 (18)	C16—C17—C12	120.22 (18)

C6—C7—H7	119.9	C16—C17—H17	119.9
C2—C7—H7	119.9	C12—C17—H17	119.9
C6—C8—H8A	109.5	C16—C18—H18A	109.5
C6—C8—H8B	109.5	C16—C18—H18B	109.5
H8A—C8—H8B	109.5	H18A—C18—H18B	109.5
C6—C8—H8C	109.5	C16—C18—H18C	109.5
H8A—C8—H8C	109.5	H18A—C18—H18C	109.5
H8B—C8—H8C	109.5	H18B—C18—H18C	109.5
O1—C9—C10	106.11 (17)	O11—C19—C20	107.04 (17)
O1—C9—H9A	110.5	O11—C19—H19A	110.3
C10—C9—H9A	110.5	C20—C19—H19A	110.3
O1—C9—H9B	110.5	O11—C19—H19B	110.3
C10—C9—H9B	110.5	C20—C19—H19B	110.3
H9A—C9—H9B	108.7	H19A—C19—H19B	108.6
C9—C10—H10A	109.5	C19—C20—H20A	109.5
C9—C10—H10B	109.5	C19—C20—H20B	109.5
H10A—C10—H10B	109.5	H20A—C20—H20B	109.5
C9—C10—H10C	109.5	C19—C20—H20C	109.5
H10A—C10—H10C	109.5	H20A—C20—H20C	109.5
H10B—C10—H10C	109.5	H20B—C20—H20C	109.5
C9—O1—C1—N1	178.80 (17)	C19—O11—C11—N11	178.92 (17)
C9—O1—C1—S1	−1.1 (3)	C19—O11—C11—S11	−0.6 (3)
C2—N1—C1—O1	−3.2 (3)	C12—N11—C11—O11	−3.8 (3)
C2—N1—C1—S1	176.68 (16)	C12—N11—C11—S11	175.77 (16)
C1—N1—C2—C3	−172.1 (2)	C11—N11—C12—C13	−147.0 (2)
C1—N1—C2—C7	7.3 (3)	C11—N11—C12—C17	35.4 (3)
C7—C2—C3—C4	0.2 (3)	C17—C12—C13—C14	−1.1 (3)
N1—C2—C3—C4	179.66 (18)	N11—C12—C13—C14	−178.82 (17)
C2—C3—C4—C5	−0.7 (3)	C12—C13—C14—C15	−0.3 (3)
C3—C4—C5—C6	0.7 (3)	C13—C14—C15—C16	0.7 (3)
C4—C5—C6—C7	−0.2 (3)	C14—C15—C16—C17	0.1 (3)
C4—C5—C6—C8	−178.83 (19)	C14—C15—C16—C18	179.80 (18)
C5—C6—C7—C2	−0.3 (3)	C15—C16—C17—C12	−1.5 (3)
C8—C6—C7—C2	178.33 (18)	C18—C16—C17—C12	178.84 (18)
C3—C2—C7—C6	0.3 (3)	C13—C12—C17—C16	2.0 (3)
N1—C2—C7—C6	−179.08 (18)	N11—C12—C17—C16	179.53 (17)
C1—O1—C9—C10	−178.76 (17)	C11—O11—C19—C20	177.42 (18)

Hydrogen-bond geometry (Å, º)

Cg1 is the centroid of the (C12–C17) ring.

D—H···*A*	*D*—H	H···*A*	*D*···*A*	*D*—H···*A*
N1—H1*N*···S11	0.87 (1)	2.62 (1)	3.4859 (16)	174 (2)
N11—H11*N*···S1	0.87 (1)	2.54 (1)	3.3985 (15)	171 (2)
C3—H3···S11	0.95	2.86	3.708 (2)	150

C13—H13···S1	0.95	2.94	3.7090 (19)	139
C17—H17···*Cg*1^{i}	0.95	2.82	3.471 (2)	127

Symmetry code: (i) −*x*+2, *y*−1/2, −*z*+1/2.